THE JOURNAL OF PHYSICAL CHEMISTRY LETTERS
A JOURNAL OF THE AMERICAN CHEMICAL SOCIETY

pubs.acs.org/JPCL

Letter

Probing Isomerization Dynamics via a Dipole-Bound State

Yuzhu Lu, Rulin Tang, Rui Zhang, and Chuangang Ning*

Cite This: J. Phys. Chem. Lett. 2022, 13, 8711−8716

Read Online

ACCESS | Metrics & More | Article Recommendations | Supporting Information

ABSTRACT: The observation of molecular isomerization dynamics is a long-standing goal in physical chemistry. The loosely bound electron in a dipole-bound state (DBS) can be a messenger for probing the isomerization of the neutral core. Here we study the isomerization dynamics of the salt dimer $(NaCl)_2$ from linear to rhombic via a DBS using cryogenic photoelectron spectroscopy in combination with ab initio calculations. Although the energy level of the DBS is below the electron affinity of the linear $(NaCl)_2$, $(NaCl)_2^-$ in its DBS can autodetach due to the linear-to-rhombic isomerization. $(NaCl)_2^-$ in the ground DBS has a relatively long lifetime of a few nanoseconds due to the quantum tunneling through a potential barrier during the transformation from linear to rhombic. In contrast, the vibrationally excited DBS has a much shorter lifetime on the order of picoseconds. The energy distribution of autodetachment electrons has an unexpected characteristic of the thermionic emission.

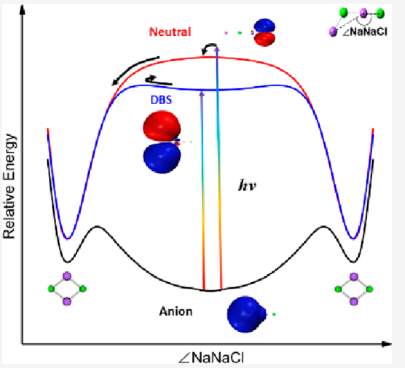

The concept of the transition state plays a defining role in a chemical reaction. The transition state often occurs at the top of a potential energy surface and acts as a reaction bottleneck, which largely determines the properties of a chemical reaction. Characterizing the transition state is a grand challenge in physical chemistry due to its fleeting nature. The photodetachment of negative ions can access transition states of specific chemical reactions.[1−5] A few benchmark reactions have been investigated by anion photodetachment spectroscopy combined with quantum dynamics calculations.[6−15] In these studies, valence-bound anions serve as the bridge to a transition state or a reaction intermedium of the neutral counterpart. A polar molecule with a large enough dipole moment (>2.5 D) can attract an extra electron to form a dipole-bound state (DBS).[16−22] The loosely bound electron occupies a diffuse molecular orbital at the positively charged end. The interaction between the DBS electron and the polar core is very weak, and the typical binding energy is around 10 meV. The potential energy surface of the dipole-bound anion is almost parallel with that of the neutral counterpart, as the neutral core is only slightly perturbed by the extra electron. Therefore, the DBS provides another way to approach the transition state. The loosely bound DBS electron can be a messenger for probing the dynamic evolution of the transition state. In this work, we report the combined study of experimental spectra and theoretical calculations, revealing the isomerization of salt dimer $(NaCl)_2^-$ via a DBS.

The simple electronic structures and large dipole moment of alkali halides make them an ideal system for studying the DBS.[23,24] The salt dimer anion $(NaCl)_2^-$ in the ground state is an open chain.[25] The potential surface around the Na−Cl−Na bending coordinate is very flat, so different theoretical methods lead to different conclusions on whether the stationary point of $(NaCl)_2^-$ is linear or slightly bent.[25−29] For the neutral $(NaCl)_2$, the ground state geometry is rhombic, and the open-chain geometry is unstable. The linear $(NaCl)_2$ has a dipole moment of about 20 D,[25] which is large enough to support several DBSs.[24] Therefore, $(NaCl)_2$ is an excellent prototype to study the structural transformation via a DBS.

Figure 1 shows the photoelectron spectrum of $(NaCl)_2^-$ acquired at photon energy $h\nu$ = 13 465 cm^{-1} using a dye laser, with the anions cooled in the ion trap at the nominal temperature of 15 K for 45 ms. It shows a series of approximately equally spaced peaks, which are the vibrational progression of the in-phase Na−Cl vibration mode with a fundamental vibrational frequency of 343(6) cm^{-1}. All peaks appear to be quite broad, and no sharp peak can be observed even if the photodetachment laser was tuned near the photodetachment threshold at the photon energy of 11 837 cm^{-1}. This confirms that the linear structure of $(NaCl)_2$ is not stable. The full-width at half-maximum (fwhm) of the first peak was measured to be 92 cm^{-1}. Generally speaking, the fwhm of a peak near the threshold is around 10 cm^{-1} for the cryogenically cooled anions on our SEVI system.[30] The broad width of the first peak is mainly due to the short lifetime of the final neutral state, giving the estimated lifetime of the neutral transition state as 58 fs. The electron affinity (EA) of linear

Received: July 29, 2022
Accepted: September 7, 2022

https://doi.org/10.1021/acs.jpclett.2c02348
J. Phys. Chem. Lett. 2022, 13, 8711−8716

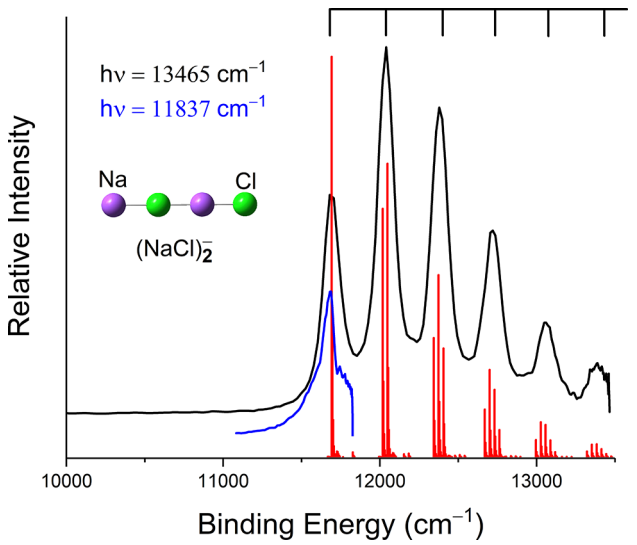

Figure 1. Photoelectron spectrum of $(NaCl)_2^-$ collected with the dye laser of $h\nu$ = 13 465 cm^{-1} at 15 K. The blue curve under the first peak is the spectrum at $h\nu$ = 11 837 cm^{-1} used for estimating the intrinsic width. The red vertical sticks are the Franck–Condon simulation.

$(NaCl)_2$ was determined to be 11 703(92) cm^{-1} or 1.451(11) eV.

To search for the DBS of $(NaCl)_2$, the photodetachment laser was scanned from the EA value 11 703 cm^{-1} down to 10 000 cm^{-1}, and the electron yield was plotted versus the photon energy. As shown in Figure 2, electrons can be

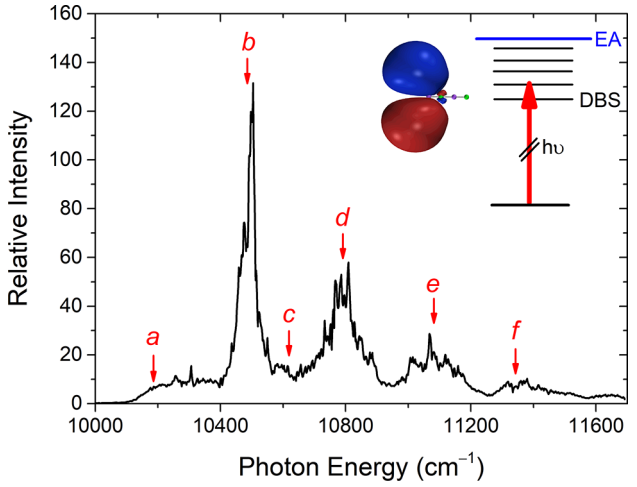

Figure 2. Photodetachment spectrum of $(NaCl)_2^-$ acquired via a DBS in the scan mode. The labels *a*–*f* indicate the photon energies used to acquire photoelectron spectra in Figure 3. The inset is the molecular orbital of the π-type DBS.

observed in a broad continuous range. Generally speaking, when the detachment photon energy is below the EA, the photoelectrons can only be produced via two-photon detachment; that is, anions are excited to the DBS by resonantly absorbing one photon and then detached by the second photon. The photodetachment spectrum usually consists of a series of sharp resonance peaks,[24,31,32] and the corresponding photoelectron energy spectrum has an enhanced peak with a very low binding energy, typically ~10 meV, equal to the binding energy of the DBS. However, the observed spectra in Figure 2 and Figure 3 have different characteristics.

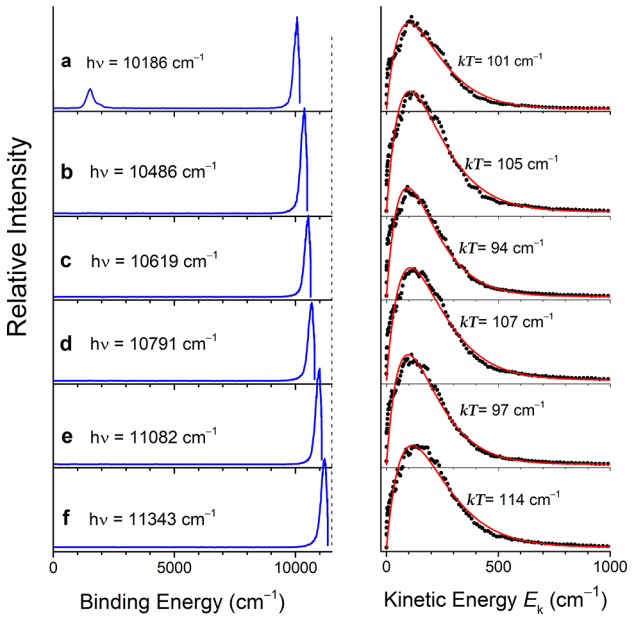

Figure 3. Photoelectron energy spectra of $(NaCl)_2^-$ plotted versus the binding energy (left) and the kinetic energy (right) at a series of photon energies. The labels of each panel are the same as those in Figure 2. The vertical dashed line is a guide for the eye. The red curves are the fitted distributions using the thermionic emission equation $f(E_k) = A\cdot(E_k/kT)\exp(-E_k/kT)$.

Instead of a sharp resonant peak as the band head, we observed a platform with an onset at 10 110 cm^{-1}. The position *a* and peaks *b* and *d*–*f* are roughly equally spaced in Figure 2, which are related to the Na–Cl vibrational progression of $(NaCl)_2^-$ in the DBS (see the Franck–Condon simulation in the Supporting Information Figure S1).

Figure 3 shows the photoelectron energy spectra of $(NaCl)_2^-$ acquired with photon energies indicated by the arrows in Figure 2. The small peak at the lower binding energy side in Figure 3(a) is contributed by the two-photon detachment via the DBS. The anisotropy parameter (β) of the peak's photoelectron angular distribution (PAD) is 0.7. Therefore, the observed DBS is π-type. A π-type DBS is rare but not a surprise for $(NaCl)_2$ because of its large dipole moment ~20 D.[20,24,33] Its binding energy was determined to be 1546(95) cm^{-1} or 192(12) meV, substantially larger than a typical value of ~10 meV. The strong peak with a higher binding energy ~10 000 cm^{-1} is an unexpected result, which did not show up in Figure 1. Its binding energy depends on the photon energy, but its kinetic energy is independent of the photon energy. This peak is due to the autodetachment of $(NaCl)_2^-$ in the DBS. It should be noted that autodetachment from the rotational or vibrational excited DBS above the EA has been well investigated during the recent decades,[31,34,35] but autodetachment of the DBS below the EA has barely been reported. The observed isotropic PAD with β = 0 also supports the autodetachment mechanism. The profiles of energy distributions of the autodetachment are quite broad and have a long tail in the higher kinetic energy region, which have the characteristics of the thermionic emission.[36,37] Therefore, the kinetic energy spectra were fitted with the equation $f(E_k)$ =

https://doi.org/10.1021/acs.jpclett.2c02348
J. Phys. Chem. Lett. 2022, 13, 8711–8716

$A\cdot(E_k/kT)\ \exp(-E_k/kT)$, where A is a constant, E_k is the kinetic energy, k is the Boltzmann constant, and T is the temperature. As shown in Figure 3, the electron kinetic spectra can be well described by the thermionic emission, and the average kinetic energy ($=2kT$) is around 200 cm^{-1}. It is unusual to see a classic thermal distribution for the autodetachment electrons from such a small molecular anion. The energy spectrum of autodetachment electrons from a DBS of cold ions usually has a sharp peak with kinetic energy related to the vibration quanta.[24,38,39]

Since the two-photon-detachment peak appears only at the band head (position *a* in Figure 2) and the intensity of autodetachment is comparable with that of the two-photon direct detachment, the lifetime of the ground DBS at position *a* should be comparable with the pulse duration of our laser system (6 ns), and the lifetimes at positions *b*–*f* should be much shorter than 6 ns. Based on the width of peak *b* in Figure 2, the lifetime for peak *b* is estimated to be on the order of picoseconds. A pump–probe type experiment can be used to accurately measure its lifetime in the future, as demonstrated by Kim group[40,41] and Verlet group[42,43] recently.

To further understand the observed results, we carried out ab initio calculations for $(NaCl)_2^-$ and $(NaCl)_2$. For neutral $(NaCl)_2$ and $(NaCl)_2^-$ in the ground state the geometries were optimized using the B3LYP functional[44] with the dispersion D3 correction.[45] The basis set def2-TZVPD[46] was adopted for all atoms. The single point energies were calculated at the CCSD(T) /aug-cc-pVTZ level.[47−49] According to our calculations, the ground state of $(NaCl)_2^-$ is linear, and the bending vibrational mode has a very low frequency of ∼10 cm^{-1} due to the flat potential. The rhombic $(NaCl)_2^-$ lies 0.179 eV above the global minimum, which is consistent with the 0.181 eV calculated by Anusiewicz et al.[25] The vertical detachment energy of $(NaCl)_2^-$ was calculated as 1.464 eV, in excellent agreement with our experimental result of 1.451(11) eV. Our calculations confirmed that the linear structure of the neutral is a transition state. The DBSs of $(NaCl)_2^-$ were calculated using the equation-of-motion coupled-cluster method for electron attachment with single and double substitutions (EOM-EA-CCSD) method.[50−52] For the linear $(NaCl)_2^-$, there are three σ-type DBSs with binding energies 184.0, 26.8, and 3.5 meV, and two π-type DBSs with binding energies 211.2 and 9.2 meV, respectively. The observed two-photon detachment in the present work is from the lowest DBS, that is, the π-type with a predicted binding energy 211.2 meV. The observed binding energy 192(12) meV and the observed PAD with $\beta = 0.7$ are consistent with the prediction of the lowest π-type DBS. To investigate the potential energy surface and the dipole moment, we scan the angle ∠NaNaCl through a restrictive optimization of $(NaCl)_2^-$ in its lowest DBS as the geometry changes from linear to rhombic. Figure 4 shows the potential energy curves of the ground state of $(NaCl)_2^-$ anion, the lowest DBS, the ground state of neutral $(NaCl)_2$, and the dipole moment (dm) curve for ground state $(NaCl)_2$. Both the potential energy curves of $(NaCl)_2^-$ in its DBS and the neutral $(NaCl)_2$ have a flat mountain top around the linear form. The DBS has a small barrier with a height 226 cm^{-1} (28 meV) between the linear structure and the closed ring. This can explain that two-photon detachment is significant for position *a*, but much weaker or disappears for positions at higher photon energy. The excited dipole-bound $(NaCl)_2^-$ can surmount the small barrier easily. Therefore, $(NaCl)_2^-$ quickly evolved from the linear structure to the rhombic one. The dipole-bound electron will be ejected during this process because the dipole moment reduces drastically. Since the autodetachment also happens at position *a*, the possible explanation is the tunneling process of the terminal Na atom with a concerted motion of the other three atoms. Compared with the intensity of peak *b*, the intensity of the autodetachment at position *a* was substantially suppressed by the barrier. The photon energy absorbed by the $(NaCl)_2^-$ is over 10 000 cm^{-1}. Suppose that the energy difference between the linear and rhombic isomers was all converted into the thermal vibrational energy of the rhombic neutral $(NaCl)_2$ in a classic way, the vibrational temperature is ∼1100 cm^{-1}/k = 1580 K, much higher than the temperature of thermionic electrons (∼100 cm^{-1}/k = 144 K). This means that electrons are not at thermal equilibrium with the atomic motion of $(NaCl)_2$ due to the fast autodetachment. The dense vibrational states at a high temperature lead to a quasi-continuum distribution for autodetachment electrons. This contrasts sharply with the discrete peaks from the autodetachment of the generic DBS with only a few vibrationally excited quanta.[24,38,39]

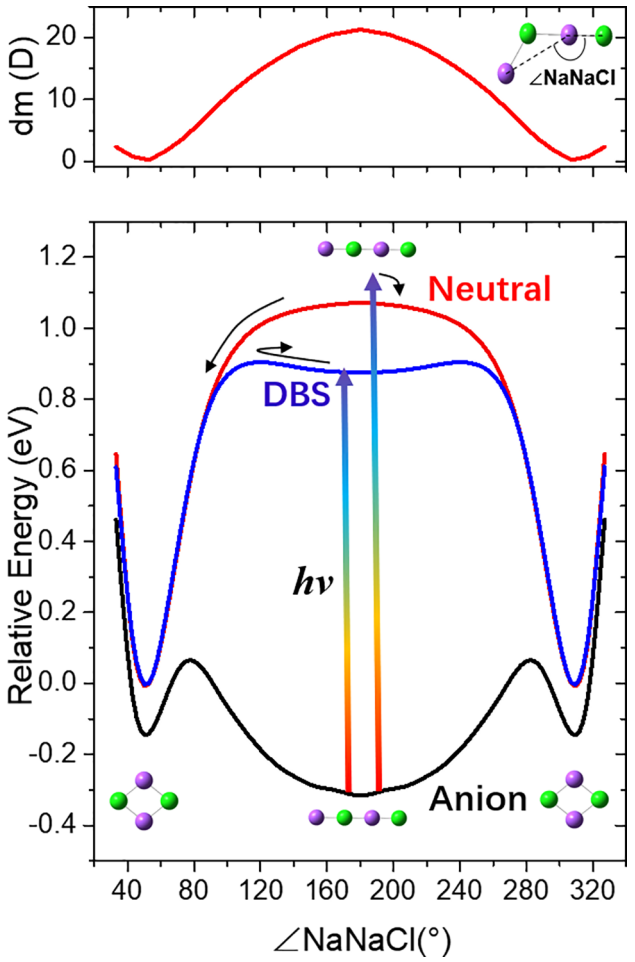

Figure 4. Dipole moment (dm) (top) and potential energy curves (bottom) of $(NaCl)_2$ versus the angle ∠NaNaCl. The red curves are for the neutral $(NaCl)_2$ in the ground state, black for $(NaCl)_2^-$ in the ground state, and blue for the lowest DBS.

Our ab initio molecular dynamics simulation shows that the linear $(NaCl)_2$ produced via photodetachment will evolve to the rhombic in 840 fs (see supplementary Figure S2). It takes 600 fs from ∠NaNaCl = 180° to 120° due to the flat potential

https://doi.org/10.1021/acs.jpclett.2c02348
J. Phys. Chem. Lett. 2022, 13, 8711−8716

surface, which is substantially slower than the Na−Cl stretching vibration with a period of 9.7 fs. This can explain why we can still observe a regular vibrational progression of the Na−Cl vibrational mode in Figure 1, although the linear $(NaCl)_2$ after photodetachment is unstable relative to the rhombic isomer.

In summary, the isomerization dynamics of the salt dimer $(NaCl)_2$ from linear to rhombic was investigated via the dipole bound state (DBS) using cryogenic photoelectron spectroscopy combined with ab initio calculations. The loosely bound DBS electron can be a messenger for probing the isomerization dynamics of the neutral core from linear to rhombic. A DBS widely exists in polar molecules. A pump−probe type experiment via a DBS will be a powerful method for investigating transition states, isomerization dynamics, and quantum thermodynamics of a small system ranging from a dimer to a nanosized cluster.

METHODS

The experiment was carried out on our slow-electron velocity-map imaging (SEVI) apparatus equipped with a cryogenically controlled ion trap.[53,54] The instrument can work in the SEVI mode or the scan mode. The SEVI mode is for acquiring the high-resolution photoelectron energy spectra, while the scan mode is for searching for resonance peaks by scanning the wavelength of the photodetachment laser.[55] The $(NaCl)_2^-$ anions were generated via laser ablation of a NaCl salt disk with helium carrier gas delivered by a pulsed valve. The generated anions were guided into the radio frequency ion trap by a hexapole ion guide, and then cooled through collisions with the buffer gas (20% H_2 and 80% He) in the ion trap. All spectra in the present work were collected with the ion trap at a nominal temperature of 15 K. The SEVI method features a very high energy resolution for low kinetic energy electrons. It can achieve an energy resolution of a few cm^{-1} near a threshold photodetachment.[54,56,57] After cooling for 45 ms, the anions were pulsed out from the cold trap, and were then analyzed in a Wiley−McLaren type time-of-flight (TOF) mass spectrometer.[58] The anions of interest were selected by a mass gate and photodetached in the interaction zone of velocity map imaging (VMI). The detachment laser was either the idler light of an optical parametric oscillator (OPO, 710−2750 nm for the idler light and line width ∼5 cm^{-1}) pumped by a Quanta-Ray Lab 190 Nd:YAG, or the tunable dye laser (400−920 nm, line width ∼0.06 cm^{-1}).

The potential energy curves of $(NaCl)_2^-$ and $(NaCl)_2$ were calculated using the coupled-cluster single−double (CCSD) method.[47] The isomerization dynamics were simulated using classic molecular dynamics. Additional theoretical details, including the Franck−Condon simulations, and molecular dynamics, are given in the Supporting Information.

ASSOCIATED CONTENT

Supporting Information

The Supporting Information is available free of charge at https://pubs.acs.org/doi/10.1021/acs.jpclett.2c02348.

Results of Franck−Condon simulations for the photodetachment spectrum, ab initio molecular dynamic of $(NaCl)_2$, detailed information on computational methods, calculated geometries and vibrational frequencies (PDF)

AUTHOR INFORMATION

Corresponding Author

Chuangang Ning − *Department of Physics, State Key Laboratory of Low Dimensional Quantum Physics, Tsinghua University, Beijing 100084, China;* orcid.org/0000-0002-3158-1253; Email: ningcg@tsinghua.edu.cn

Authors

Yuzhu Lu − *Department of Physics, State Key Laboratory of Low Dimensional Quantum Physics, Tsinghua University, Beijing 100084, China*

Rulin Tang − *Department of Physics, State Key Laboratory of Low Dimensional Quantum Physics, Tsinghua University, Beijing 100084, China*

Rui Zhang − *Department of Physics, State Key Laboratory of Low Dimensional Quantum Physics, Tsinghua University, Beijing 100084, China;* orcid.org/0000-0001-9080-4528

Complete contact information is available at: https://pubs.acs.org/10.1021/acs.jpclett.2c02348

Notes

The authors declare no competing financial interest.

ACKNOWLEDGMENTS

This work is supported by the National Natural Science Foundation of China (NSFC) (Grant No. 11974199) and the National key R&D program of China (2018YFA0306504).

REFERENCES

(1) Neumark, D. M. Transition-state spectroscopy via negative ion photodetachment. *Acc. Chem. Res.* **1993**, *26*, 33−40.

(2) Neumark, D. M. Transition State Spectroscopy. *Science* **1996**, *272*, 1446−1447.

(3) Continetti, R. E.; Guo, H. Dynamics of transient species via anion photodetachment. *Chem. Soc. Rev.* **2017**, *46*, 7650−7667.

(4) Continetti, R. E. The view from a transition state. *Nat. Chem.* **2017**, *9*, 931−932.

(5) Neumark, D. M. Probing the transition state with negative ion photodetachment: experiment and theory. *Phys. Chem. Chem. Phys.* **2005**, *7*, 433−442.

(6) DeVine, J. A.; Weichman, M. L.; Laws, B.; Chang, J.; Babin, M. C.; Balerdi, G.; Xie, C.; Malbon, C. L.; Lineberger, W. C.; Yarkony, D. R.; et al. Encoding of vinylidene isomerization in its anion photoelectron spectrum. *Science* **2017**, *358*, 336−339.

(7) Weichman, M. L.; DeVine, J. A.; Babin, M. C.; Li, J.; Guo, L.; Ma, J.; Guo, H.; Neumark, D. M. Feshbach resonances in the exit channel of the F + CH_3OH → HF + CH_3O reaction observed using transition-state spectroscopy. *Nat. Chem.* **2017**, *9*, 950−955.

(8) Wenthold, P. G.; Hrovat, D. A.; Borden, W. T.; Lineberger, W. C. Transition-State Spectroscopy of Cyclooctatetraene. *Science* **1996**, *272*, 1456−1459.

(9) Chen, B.; Hrovat, D. A.; West, R.; Deng, S. H. M.; Wang, X.-B.; Borden, W. T. The Negative Ion Photoelectron Spectrum of Cyclopropane-1,2,3-Trione Radical Anion, $(CO)3^{\bullet-}$ — A Joint Experimental and Computational Study. *J. Am. Chem. Soc.* **2014**, *136*, 12345−12354.

(10) Kim, J. B.; Weichman, M. L.; Sjolander, T. F.; Neumark, D. M.; Kłos, J.; Alexander, M. H.; Manolopoulos, D. E. Spectroscopic observation of resonances in the F + H_2 reaction. *Science* **2015**, *349*, 510−513.

(11) Wheeler, M. D.; Anderson, D. T.; Lester, M. I. Probing reactive potential energy surfaces by vibrational activation of H_2-OH entrance channel complexes. *Int. Rev. Phys. Chem.* **2000**, *19*, 501−529.

(12) Otto, R.; Ma, J.; Ray, A. W.; Daluz, J. S.; Li, J.; Guo, H.; Continetti, R. E. Imaging Dynamics on the F + H_2O → HF + OH

Potential Energy Surfaces from Wells to Barriers. *Science* **2014**, *343*, 396−399.
(13) Lester, M. I.; Pond, B. V.; Marshall, M. D.; Anderson, D. T.; Harding, L. B.; Wagner, A. F. Mapping the OH + CO → HOCO reaction pathway through IR spectroscopy of the OH−CO reactant complex. *Faraday Discuss.* **2001**, *118*, 373−385.
(14) Clements, T. G.; Continetti, R. E.; Francisco, J. S. Exploring the OH+CO→H+CO_2 potential surface via dissociative photodetachment of $(HOCO)^-$. *J. Chem. Phys.* **2002**, *117*, 6478−6488.
(15) Lu, Z.; Hu, Q.; Oakman, J. E.; Continetti, R. E. Dynamics on the HOCO potential energy surface studied by dissociative photodetachment of $HOCO^-$ and $DOCO^-$. *J. Chem. Phys.* **2007**, *126*, 194305.
(16) Compton, R.; Hammer, N. Multipole-Bound Molecular Anions. In *Advances in Gas-Phase Ion Chemistry*; Adams, N., Babcock, L., Eds.; Elsevier: New York, 2001; Vol. *4*, pp 257−291.
(17) Liu, G.; Ciborowski, S. M.; Pitts, C. R.; Graham, J. D.; Buytendyk, A. M.; Lectka, T.; Bowen, K. H. Observation of the dipole- and quadrupole-bound anions of 1,4-dicyanocyclohexane. *Phys. Chem. Chem. Phys.* **2019**, *21*, 18310−18315.
(18) Liu, G.; Ciborowski, S. M.; Graham, J. D.; Buytendyk, A. M.; Bowen, K. H. Photoelectron spectroscopic study of dipole-bound and valence-bound nitromethane anions formed by Rydberg electron transfer. *J. Chem. Phys.* **2020**, *153*, 044307.
(19) DesfranÇOis, C.; Abdoul-Carime, H.; Schermann, J.-P. GROUND-STATE DIPOLE-BOUND ANIONS. *Int. J. Mod. Phys. B* **1996**, *10*, 1339−1395.
(20) Jordan, K. D.; Wang, F. Theory of Dipole-Bound Anions. *Annu. Rev. Phys. Chem.* **2003**, *54*, 367−396.
(21) Simons, J. Molecular Anions. *J. Phys. Chem. A* **2008**, *112*, 6401−6511.
(22) Qian, C.-H.; Zhu, G.-Z.; Wang, L.-S. Probing the Critical Dipole Moment To Support Excited Dipole-Bound States in Valence-Bound Anions. *J. Phys. Chem. Lett.* **2019**, *10*, 6472−6477.
(23) Gutsev, G. L.; Nooijen, M.; Bartlett, R. J. Valence and excited dipole-bound states of polar diatomic anions: LiH^-, LiF^-, $LiCl^-$, NaH^-, NaF^-, $NaCl^-$, BeO^-, and MgO^-. *Chem. Phys. Lett.* **1997**, *276*, 13−19.
(24) Lu, Y.; Tang, R.; Ning, C. Observation of an Excited Dipole-Bound State in a Diatomic Anion. *J. Phys. Chem. Lett.* **2021**, *12*, 5897−5902.
(25) Anusiewicz, I.; Skurski, P.; Simons, J. First Evidence of Rhombic $(NaCl)_2^-$. Ab Initio Reexamination of the Sodium Chloride Dimer Anion. *J. Phys. Chem. A* **2002**, *106*, 10636−10644.
(26) Sunil, K. K.; Jordan, K. D. Negative ion formation in alkali halide clusters. *J. Phys. Chem.* **1987**, *91*, 1710−1711.
(27) Sunil, K. K.; Jordan, K. D. Theoretical study of the $NaClNaCl^-$ ↔ $ClNaNaCl^-$ interconversion. *Chem. Phys. Lett.* **1989**, *164*, 509−513.
(28) Xia, P.; Yu, N.; Bloomfield, L. A. Experimental and theoretical studies of single excess electrons in sodium chloride cluster anions. *Phys. Rev. B* **1993**, *47*, 10040−10043.
(29) Yu, N.; Xia, P.; Bloomfield, L. A.; Fowler, M. Structure and electron localization of anionic NaCl clusters with excess electrons. *J. Chem. Phys.* **1995**, *102*, 4965−4972.
(30) Lu, Y.; Ning, C. Structural Versatility and Energy Difference of Salt−Water Complex NaCl(H2O) Encoded in Cryogenic Photoelectron Spectroscopy. *J. Phys. Chem. Lett.* **2022**, *13*, 4995−5000.
(31) Lykke, K. R.; Neumark, D. M.; Andersen, T.; Trapa, V. J.; Lineberger, W. C. Autodetachment spectroscopy and dynamics of $CH2CN^-$ and $CD2CN^-$. *J. Chem. Phys.* **1987**, *87*, 6842−6853.
(32) Lu, Y.; Tang, R.; Fu, X.; Liu, H.; Ning, C. Dipole-bound and valence excited states of AuF anions via resonant photoelectron spectroscopy. *J. Chem. Phys.* **2021**, *154*, 074303.
(33) Yuan, D.-F.; Liu, Y.; Qian, C.-H.; Zhang, Y.-R.; Rubenstein, B. M.; Wang, L.-S. Observation of a π-Type Dipole-Bound State in Molecular Anions. *Phys. Rev. Lett.* **2020**, *125*, 073003.
(34) Laws, B. A.; Levey, Z. D.; Schmidt, T. W.; Gibson, S. T. Velocity Map Imaging Spectroscopy of the Dipole-Bound State of CH2CN−: Implications for the Diffuse Interstellar Bands. *J. Am. Chem. Soc.* **2021**, *143*, 18684−18692.
(35) Zhu, G.-Z.; Wang, L.-S. High-resolution photoelectron imaging and resonant photoelectron spectroscopy via noncovalently bound excited states of cryogenically cooled anions. *Chem. Sci.* **2019**, *10*, 9409−9423.
(36) Troe, J.; Miller, T. M.; Viggiano, A. A. On the accuracy of thermionic electron emission models. I. Electron detachment from $SF6^-$. *J. Chem. Phys.* **2009**, *130*, 244303.
(37) Andersen, J.; Bonderup, E.; Hansen, K. Thermionic emission from clusters. *J. Phys. B: At., Mol. Opt. Phys.* **2002**, *35*, R1.
(38) Liu, H.-T.; Ning, C.-G.; Huang, D.-L.; Wang, L.-S. Vibrational Spectroscopy of the Dehydrogenated Uracil Radical by Autodetachment of Dipole-Bound Excited States of Cold Anions. *Angew. Chem., Int. Ed.* **2014**, *53*, 2464−2468.
(39) Liu, H.-T.; Ning, C.-G.; Huang, D.-L.; Dau, P. D.; Wang, L.-S. Observation of Mode-Specific Vibrational Autodetachment from Dipole-Bound States of Cold Anions. *Angew. Chem., Int. Ed.* **2013**, *52*, 8976−8979.
(40) Kang, D. H.; An, S.; Kim, S. K. Real-Time Autodetachment Dynamics of Vibrational Feshbach Resonances in a Dipole-Bound State. *Phys. Rev. Lett.* **2020**, *125*, 093001.
(41) Kang, D. H.; Kim, J.; Noh, H.-R.; Kim, S. K. Observation of the ponderomotive effect in non-valence bound states of polyatomic molecular anions. *Nat. Commun.* **2021**, *12*, 7098.
(42) Rogers, J. P.; Anstöter, C. S.; Verlet, J. R. R. Ultrafast dynamics of low-energy electron attachment via a non-valence correlation-bound state. *Nat. Chem.* **2018**, *10*, 341−346.
(43) Bull James, N.; Verlet Jan, R. R. Observation and ultrafast dynamics of a nonvalence correlation-bound state of an anion. *Sci. Adv.* **2017**, *3*, No. e1603106.
(44) Stephens, P. J.; Devlin, F. J.; Chabalowski, C. F.; Frisch, M. J. Ab Initio Calculation of Vibrational Absorption and Circular Dichroism Spectra Using Density Functional Force Fields. *J. Phys. Chem.* **1994**, *98*, 11623−11627.
(45) Grimme, S.; Antony, J.; Ehrlich, S.; Krieg, H. A consistent and accurate ab initio parametrization of density functional dispersion correction (DFT-D) for the 94 elements H-Pu. *J. Chem. Phys.* **2010**, *132*, 154104.
(46) Weigend, F.; Ahlrichs, R. Balanced basis sets of split valence, triple zeta valence and quadruple zeta valence quality for H to Rn: Design and assessment of accuracy. *Phys. Chem. Chem. Phys.* **2005**, *7*, 3297−3305.
(47) Pople, J. A.; Head-Gordon, M.; Raghavachari, K. Quadratic configuration interaction. A general technique for determining electron correlation energies. *J. Chem. Phys.* **1987**, *87*, 5968−5975.
(48) Woon, D. E.; Dunning, T. H. Gaussian basis sets for use in correlated molecular calculations. III. The atoms aluminum through argon. *J. Chem. Phys.* **1993**, *98*, 1358−1371.
(49) Prascher, B. P.; Woon, D. E.; Peterson, K. A.; Dunning, T. H.; Wilson, A. K. Gaussian basis sets for use in correlated molecular calculations. VII. Valence, core-valence, and scalar relativistic basis sets for Li, Be, Na, and Mg. *Theor. Chem. Acc.* **2011**, *128*, 69−82.
(50) Krylov, A. I. Equation-of-Motion Coupled-Cluster Methods for Open-Shell and Electronically Excited Species: The Hitchhiker's Guide to Fock Space. *Annu. Rev. Phys. Chem.* **2008**, *59*, 433−462.
(51) Nooijen, M.; Bartlett, R. J. Equation of motion coupled cluster method for electron attachment. *J. Chem. Phys.* **1995**, *102*, 3629−3647.
(52) Sneskov, K.; Christiansen, O. Excited state coupled cluster methods. *WIREs Comput. Mol. Sci.* **2012**, *2*, 566−584.
(53) Luo, Z.; Chen, X.; Li, J.; Ning, C. Precision measurement of the electron affinity of niobium. *Phys. Rev. A* **2016**, *93*, 020501.
(54) Tang, R.; Fu, X.; Ning, C. Accurate electron affinity of Ti and fine structures of its anions. *J. Chem. Phys.* **2018**, *149*, 134304.
(55) Tang, R.; Si, R.; Fei, Z.; Fu, X.; Lu, Y.; Brage, T.; Liu, H.; Chen, C.; Ning, C. Observation of electric-dipole transitions in the laser-cooling candidate Th^- and its application for cooling antiprotons. *Phys. Rev. A* **2021**, *103*, 042817.

https://doi.org/10.1021/acs.jpclett.2c02348
J. Phys. Chem. Lett. 2022, 13, 8711−8716

(56) Hock, C.; Kim, J. B.; Weichman, M. L.; Yacovitch, T. I.; Neumark, D. M. Slow photoelectron velocity-map imaging spectroscopy of cold negative ions. *J. Chem. Phys.* **2012**, *137*, 244201.
(57) León, I.; Yang, Z.; Liu, H.-T.; Wang, L.-S. The design and construction of a high-resolution velocity-map imaging apparatus for photoelectron spectroscopy studies of size-selected clusters. *Rev. Sci. Instrum.* **2014**, *85*, 083106.
(58) Wiley, W. C.; McLaren, I. H. Time-of-Flight Mass Spectrometer with Improved Resolution. *Rev. Sci. Instrum.* **1955**, *26*, 1150−1157.

https://doi.org/10.1021/acs.jpclett.2c02348
J. Phys. Chem. Lett. 2022, 13, 8711−8716